Contaminant migration in unsaturated porous media using X-ray computerized tomography (CT)

Nian Qing Zhou, Shan Zhao, Wei Song and Jun Otani

ABSTRACT

Landfills are usually located in unsaturated zones. Contaminant leaking can easily infiltrate groundwater through these porous media and contribute to groundwater pollution. The main objective of this work is to study the leachate migration in unsaturated porous media using X-ray computerized tomography (CT) and image-processing software. Silica sand and Yamazuna sand (collected from Japan) with different particle sizes are considered. Potassium iodide (KI) solution is used as a contaminant and injected into sand specimens at appropriate rates. The specimens are scanned at each cross section before and after contaminant injection by X-ray CT. Subsequently, all CT images are transformed into mean CT values by Image J software. VGStudio software is then used to reconstruct the subtracted images into three-dimensional images. The results indicate that vertical migration is dominant in uniform sand and horizontal migration is the main behavior in well-graded sand. Meanwhile, it is also confirmed that CT scanning is an effective technology to study contaminant migration in unsaturated porous media with different grain sizes.

Key words | computerized tomography (CT), contaminant migration, image-processing software, leachate, mean CT value

Nian Qing Zhou (corresponding author)
Shan Zhao
Department of Hydraulic Engineering,
Tongji University,
Shanghai 200092,
China
and
Key Laboratory of Yangtze River Water Environment,
Ministry of Education,
China
E-mail: *nq.zhou@tongji.edu.cn*

Wei Song
Jun Otani
Department of Civil and Environmental Engineering,
Kumamoto University,
Kumamoto 8608555,
Japan

INTRODUCTION

Landfills are very important in solid waste treatment for metropolitan areas. Many landfills are located in unsaturated porous zones and the induced contaminant leaking has caused serious environmental problems. Landfill leachate is generated from excess rainwater percolating through waste, representing a potential risk to groundwater and surface water. Nowadays, the composition and treatment of landfill leachate in unsaturated porous media has gained some recognition; however, the experimental determination of pollution plumes still remains a problem, because conventional methods of subsurface contamination investigation are costly and technically complicated (Wittlingerova *et al.* 2013). In contrast, laboratory experiments are a direct and effective way to study contaminant migration, because boundary conditions and the properties of soils and contaminants can be easily controlled.

The issue of contaminant migration in unsaturated zones has been extensively studied by many scholars (e.g. Bunsri *et al.* 2009), especially in the context of landfill leachate pollution (Baumann *et al.* 2006; Slack *et al.* 2007). Previous studies have noted that the development of a method to identify leachate migration in unsaturated zones is of great significance. However, few efficient experimental methods for the investigation and visualization of leachate migration in porous media have been fully developed, limiting our understanding of the effects of leachate on the environment. Currently, studying leachate migration using only statistical techniques is very challenging because effective strategies or analytical techniques may be insufficient for detecting pollutants at a low concentration (Mouser *et al.* 2010). Fortunately, technological development has allowed more applications relevant to contaminant migration. Werth *et al.* (2010) presented four non-invasive imaging methods, including X-ray microtomography etc., to review the theory of these methods and their applications to contaminant migration research. Computerized tomography (CT) is a nondestructive technique that allows visualization of the internal structure of objects, determined mainly by variations in density and atomic composition (Mees *et al.* 2003). It can be employed to examine the nature of contaminant movement in soils in real time.

doi: 10.2166/wst.2013.801

Thus, this paper focuses on the modeling of imitative leachate migration in unsaturated porous media using CT and image-processing software. Potassium iodide (KI) solution is selected as the leachate in this study. A series of tests are conducted and the behaviors of KI migration in two types of sand specimens are scanned before and after the injection using X-ray CT. A large number of CT images and data are obtained. Based on the results, patterns of KI migration in sand with different particle sizes are evaluated. The conclusions derived from this study may provide a scientific basis for pollution monitoring and environmental evaluation. This also confirms that the X-ray CT method is effective for engineering purposes.

METHODS AND MATERIALS

Foundations of CT scanner

The CT scanner used in this experiment is a TOSHIBA Corp. TOSCANER-23200min, provided by the CT Laboratory of the X-Earth Research Center in Kumamoto University, Japan. CT value is used as a measure of the degree of X-ray attenuation by a material: the greater the CT number, the greater the attenuation. The comprehensive knowledge of CT is taken from Hounsfield (1973).

For the CT image, which is constructed in three dimensions, voxels are used as the image unit instead of pixels. Thus, the resolution of the CT scanner is given in voxels. The CT value can be defined as the density in each voxel. A voxel size of 0.293 mm × 0.293 mm × 1 mm is used in this study, identical to that in Eskisar *et al.* (2012). Specifically, if a soil particle is larger than a single voxel, the obtained value can be realized as the soil particle density. However, if the soil particle is smaller than a single voxel, the resultant CT value is an averaged density including both the soil particle and the surrounding void.

Specimen selection

The silica and Yamazuna sand specimens used in this experiment are taken from Kumamoto (Japan). Silica sand is uniform, more round and has an even particle-size distribution. In contrast, Yamazuna sand is typically heterogeneous, with an uneven particle-size distribution. The main physical and mechanical indexes are listed in Table 1.

Specimen preparation

First, a 1.5-cm-thick gravel layer is placed at the bottom of a transparent cylindrical container (20 cm inner diameter). After leveling the gravel layer, 0.5-mm-thick geotextile is laid on top. Next, the container is filled with sand specimens by sieving. To minimize the effect of sieve height on specimen uniformity, four 10-cm height levels are adopted. A plastic pipe equipped with a control switch connects the bottom of the container and the tank with a constant water head. Prior to the experiment, the switch is turned off, the container is placed on a weighing machine and the water tank is adjusted to maintain the water level and keep the bottom of the sand specimens at the same level. After completion of preparation work, the gravel layer is saturated with the switch open. The water rises along the pores due to capillary force for more than ten hours until the weighing machine reading remains unchanged. Thus, the water content is in a stable unsaturated state (Figure 1).

Determination of the specimen saturation

The two sand types have extremely different particle-size distributions and heterogeneous pore sizes, both of which result in different capillary rise heights. Two groups of tests are conducted for each type of sand to determine the capillary rise height (Table 2). The maximum capillary rise height after 5, 10, 20, 30 and 60 min (using the container bottom as the reference) was recorded, and measurements were then taken every hour until the height remained constant. Throughout the specimen preparation, the top of container was sealed by a cover layer to minimize the evaporation of the water in the sand. Two different heights are required to achieve the stable unsaturated state: 235 and 380 mm for silica and Yamazuna sand, respectively. This

Table 1 | Physical and mechanical parameters of the specimens

Sample name	Specific gravity (γ/kN m^{-3})	Specific weight (G)	Maximum dry density	Porosity ratio (e)	Coefficient of uniformity (C_u)	Coefficient of curvature (C_c)
Silica	15.48	2.633	1.578	0.67	1.60	0.96
Yamazuna	15.98	2.695	1.629	0.65	12.00	1.23

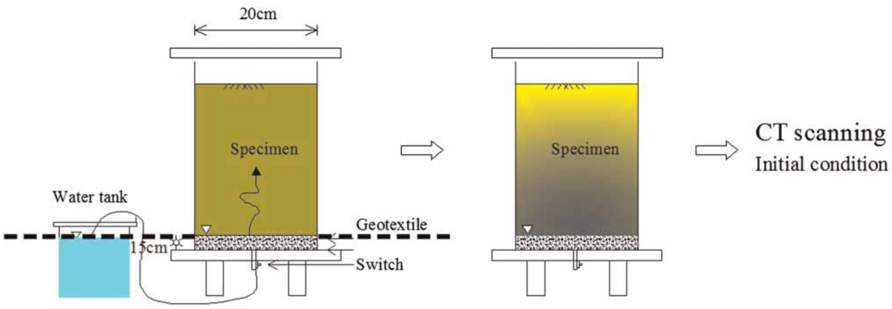

Figure 1 | Schematic diagram of apparatus.

setup provides a scientific basis for studying contaminant migration in unsaturated porous media.

Scanning initial specimens

The CT scanner with set parameters is used to scan each layer of the specimens. Image artifacts derived from beam hardening are a common issue in X-ray CT. However, beam-hardening artifacts can be reduced by the application of certain measures (Ketcham & Carlson 2001). Several efficient approaches are used to minimize the image artifacts in this case: removing the outer edge of the initial image during image reconstruction; setting the scanning voltage for the X-ray tube to 300 kV, as suggested by Otani *et al.* (2000); and scanning the empty transparent container in advance to eliminate the effect of air and transparent materials on X-ray absorption. The specimens in the CT room (Figure 2) were rotated 360° and scanned by a 1.0-mm-thick X-ray beam to obtain the original image. For each experiment, the scanned slice thickness is 5 mm and a complete 360° scan requires 8 minutes per slice. Initial images in the two specimens are given in Figure 3. In CT images, the dark and light areas are low-density and high-density zones, respectively. The shade of the upper-row images is the deepest, indicating that the corresponding sand has the lowest density. With increasing scanning depth, the CT images become increasingly light in shade, indicating that the specimen density increases. This increase is due to the higher moisture content of the spaces between particles, accordingly, the lower air content, both of which increase the specimen density.

After the scanning of the initial specimen, Image J is used to calculate the mean CT value of each scanning layer; the corresponding saturation of each layer is also measured to obtain the relationships between them (Figure 4).

Table 2 | Specimen parameters and capillary rise height in capillary experiment

Specimen No.	Control density (ρ_d/g/cm^3)	Specimen	Time (h)	Height of capillary rise (mm)
TG1	1.563	Silica	42	230
TG2	1.578	Silica	45	235
TS1	1.629	Yamazuna	112	375
TS2	1.633	Yamazuna	112	380

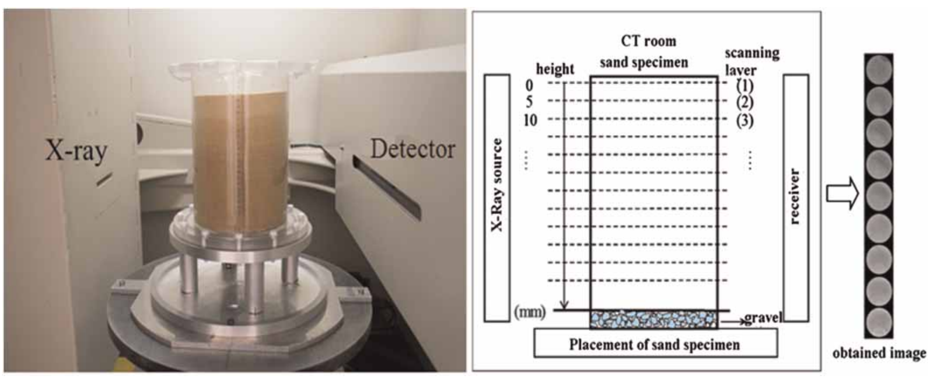

Figure 2 | The photograph and scheme of the specimen in CT room.

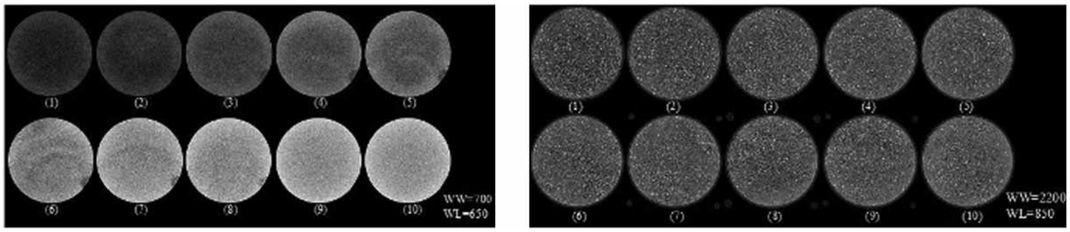

Figure 3 | Silica sand (left) and Yamazuna sand (right) CT images under initial conditions.

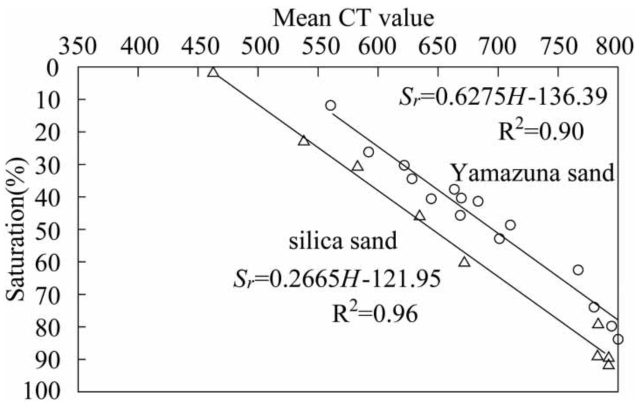

Figure 4 | The fitted linear of mean CT values vs. saturation.

Contaminant injection

An injector ($\Phi = 0.1$ mm) filled with KI solution is placed above the prepared stable unsaturated sand specimens. A switch is used to control the injection time. KI solution is selected as the contaminant in this study due to its wide availability, relative safety and high solubility in water (Altman *et al.* 2005). Generally, the concentration of newly produced leachate is very high, mainly containing four groups of pollutants (dissolved organic matter, inorganic macrocomponents, heavy metals, and xenobiotic organic compounds) (Kjeldsen *et al.* 2002). Potassium (K+) is one of most common inorganic macrocomponents in leachate. As a non-reactive tracer, iodide is thought to have a minimal reaction with geological media and is often used to evaluate advection, dispersion and diffusion (Zhelezny & Shapiro 2006). More importantly, iodide can be easily detected by X-rays used in CT. Considering sorption to mineral surfaces and advection, a density of 1.1 g/cm^3 is accurately prepared, under which conditions the migration plume can be observed clearly and precisely. Throughout the process, the KI solution is injected uniformly at 0.69 g/s.

An intermittent injection method is used in this study to simulate landfill leaching. The experimental sequences are as follows: the switch is opened and the KI solution is injected continuously for 13.5 s, then the switch is closed, followed by a scan of each layer from the top downward. Each scanning slice thickness is also 5 mm. After completion of the scanning, the switch is reopened and the KI solution is injected for 20.0 s, before being closed again, and then scanning the same layer from the top downward. The above-mentioned operations are repeated for injection times of 31.4, 43.0, 60.0, 93.4 and 182.6 s. Finally, the scanning images for each cross section are obtained. Here, only the top five layer images are presented in Figure 5.

The three-dimensional images are reconstructed by VGStudio, which is professional-grade software that generates a volume model from voxel data. Figure 6(a) is a reconstructed image profile of sand specimens. VGStudio has high precision

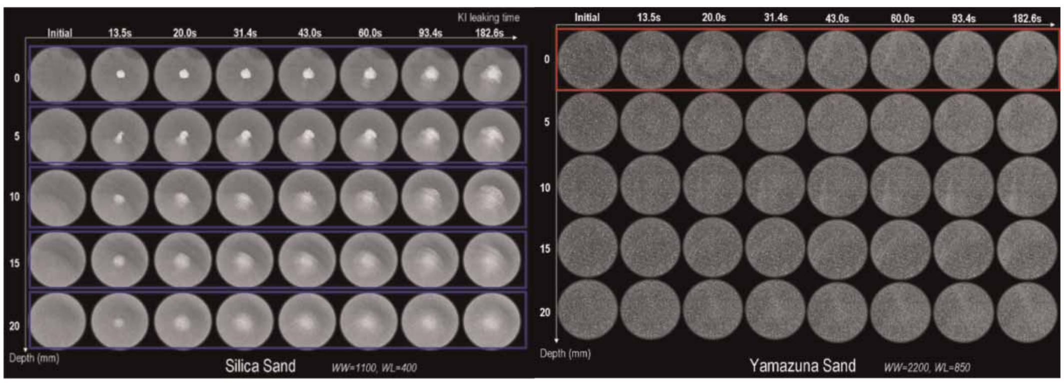

Figure 5 | CT scanning image after contaminant injection (only top five layers).

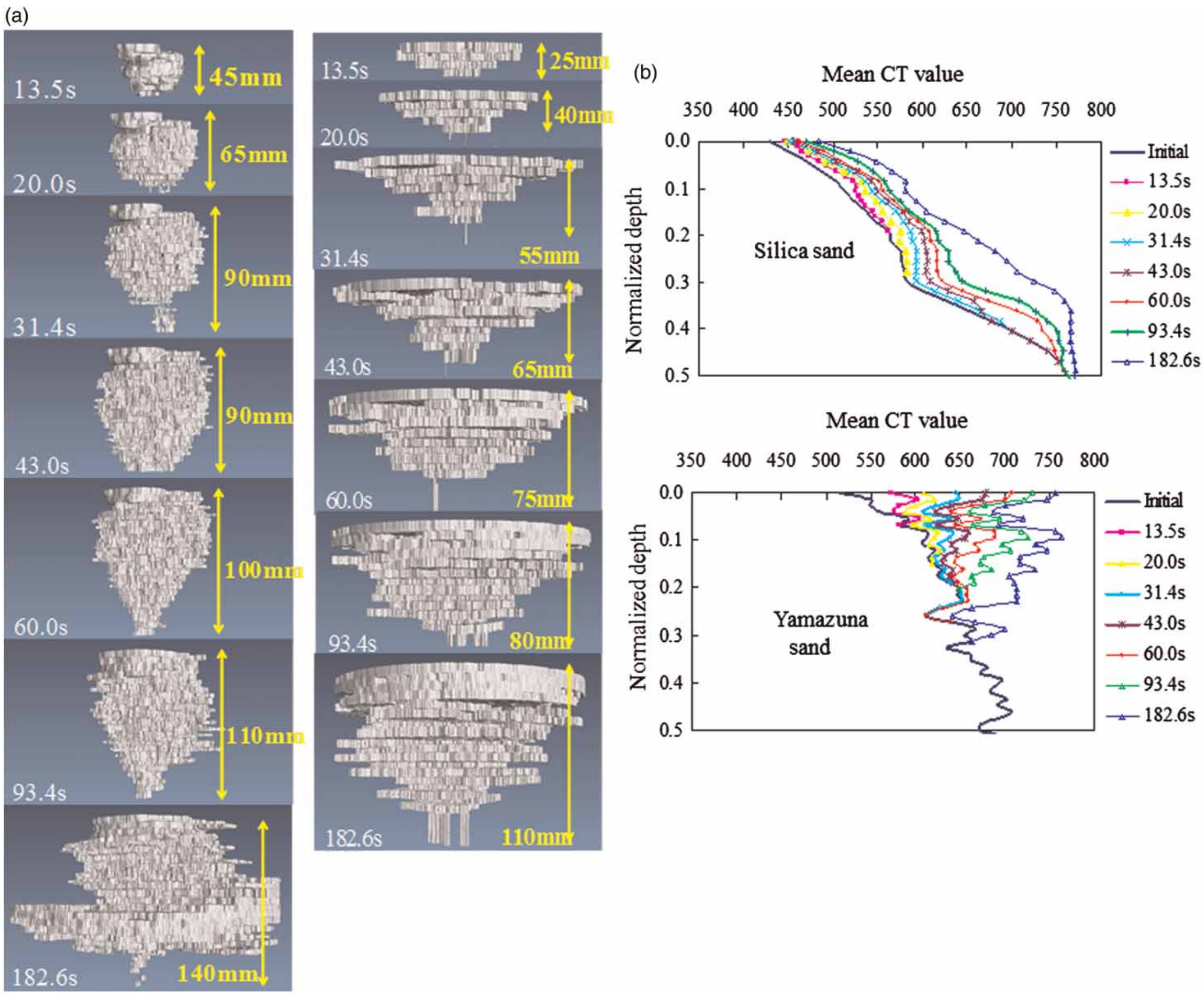

Figure 6 | (a) 3D-reconstruction images by VGStudio generated from individual CT scanner slice image data. Silica sand (left) Yamazuna sand (right); (b) The migration results of KI with depths and time in sand specimens.

and mass data processing features and can generate various three-dimensional images from the CT data. The stereogram clearly shows the KI solution migration process in the sand.

Subsequently, Figure 6(a) shows the transformation into mean CT values after image reconstruction, providing the mean CT values of KI migration with time and depth in silica sand and Yamazuna sand (Figure 6(b)).

RESULTS AND DISCUSSION

Mean CT values versus specimen saturation

The scattering points of the mean CT values versus specimen saturation are approximately linear, as shown in Figure 4. Based on the least square method, the following relationships between the mean CT value and saturation are obtained:

Silica sand $$S_r = 0.2665H - 121.95 \qquad R^2 = 0.96 \qquad (1)$$

Yamazuna sand $$S_r = 0.2675H - 136.39 \qquad R^2 = 0.90 \qquad (2)$$

where S_r is the saturation and H represents the mean CT value.

Equations (1) and (2) confirm that there is a linear relationship between the CT value and the material density. Notably, this relationship depends on scanning conditions, such as X-ray attenuation and the size and shape of the scanning materials. Therefore, the size and shape of scanning materials must be fixed for all comparative studies. In addition, the empirical formulas obtained in this experiment have certain limitations for other geomaterials, it is necessary to adjust the settings appropriately and determine the relationship through experiments.

Image analysis

According to the scanning and processing results, as noted in Figure 3, the scanning image shade from the top downward in the silica sand specimen varies from deep to shallow and from dark to light prior to the contaminant injection. This result indicates that the specimen density increases dramatically from the top downward, whereas the Yamazuna sand shade barely changes, indicating that its density changes little. Figure 5 shows that the plume of contaminant migration in the silica sand increases with increasing depth and time after the contaminant injection. In contrast, the highlights in the Yamazuna sand barely change.

The image profiles after VGStudio processing (Figure 6(a)) are more intuitive for observing KI solution migration in specimens. As shown, the contaminant migrates vertically in silica sand with relative ease but tends to migrate horizontally in Yamazuna sand. This phenomenon is attributed to the strong difference between the saturation and particle-size distributions of the two sands.

Mean CT values versus normalized depth

Figure 6(b) shows that temporal and spatial contaminant migration is quantified by the mean CT value in the silica and Yamazuna sand specimens. Clearly, the changes in the mean CT values with normalized height differ significantly. For silica sand, the mean CT value on the top of the specimen is 430 before contaminant injection and 480 after injection. All mean CT values are approximately 760 after the experiment is finished. Thus, the variation in the mean CT values with normalized height is linear, i.e., as the normalized height increases, the mean CT values also increase. In contrast, for Yamazuna sand, the change is disordered. The vertical infiltration rate in the silica sand is faster than that in the Yamazuna sand within the same timeframe; but the horizontal spread of pollution in the silica sand is smaller. This behavior is mainly determined by the large size gradation and porosity of the two sand specimens. The sensitivity of CT values clearly decreases when the saturation reaches a certain value due to the dilution of the contaminant by water.

Contaminant migration in unsaturated porous media is mainly affected by the permeability coefficient of the media. In the bottom of the specimen where the moisture content is highest, the sand is approximately 95% saturated and the permeability coefficient of it is the largest. With the decrease in moisture content, more and more pore space is filled with air, making the negative pressure increase while the permeability coefficient declines. Therefore, the increase of moisture content will enlarge the permeability coefficient of an unsaturated sand specimen. This has also been confirmed by other experiments (Li *et al.* 2004; Sun *et al.* 2004). Contaminants migrate more easily in media with a larger permeability coefficient. Consequently, the increase of saturation is conducive to contaminant migration in unsaturated porous media.

CONCLUSION

A method for obtaining accurate information regarding leachate migration in unsaturated porous media was established using CT images. The results provide a scientific basis for contaminant migration in unsaturated porous media for further numerical modeling. The following practically significant conclusions may be drawn:

(1) The saturation of sand specimens is important for the contaminant migration process. The migration speed in the unsaturated media is decided by saturation. Lower saturation will make contaminants migrate almost only as a result of the effect of gravity, which is slower than that in higher saturation.
(2) The size gradation of sands has different effects on the contaminant migration process. Uniform sand particles are beneficial to vertical contaminant migration, whereas well-graded sand increases transverse diffusion.
(3) Temporal and spatial contaminant migration in silica sand and Yamazuna sand specimens can be precisely represented by the mean CT value. X-ray CT scan technology can also be applied to study pollution characteristics in different environments. It has more benefits than conventional analyses of soil structure and can be an effective tool for examining contaminant migration in unsaturated porous media.
(4) CT scanning certainly has limitations to wider applications in engineering. Further work using CT will involve the combination of laboratory experiments

and numerical modeling. Results obtained from scanning can be used to calibrate numerical models.

ACKNOWLEDGEMENTS

This study is supported by the National Science Fund of China (No. 41272249), the Research Fund for the Doctoral Program of Higher Education of China (No. 20110072110020). The authors would also like to thank the X-Earth Research Center of Kumamoto University for supplying excellent experimental conditions.

REFERENCES

Altman, S. J., Peplinski, W. J. & Rivers, M. L. 2005 Evaluation of synchrotron X-ray computerized microtomography for the visualization of transport processes in low-porosity materials. *J. Cont. Hydrol.* **78** (3), 167–183.

Baumann, T., Fruhstorfer, P., Klein, T. & Niessner, R. 2006 Colloid and heavy metal transport at landfill sites in direct contact with groundwater. *Water Res.* **40** (14), 2776–2786.

Bunsri, T., Sivakumar, M. & Hagare, D. 2009 Transport and biotransformation of organic carbon and nitrate compounds in unsaturated soil conditions. *Water Sci. Technol.* **58** (11), 2143–2153.

Eskisar, T., Otani, J. & Hironaka, J. 2012 Visualization of soil arching on reinforced embankment with rigid pile foundation using X-ray CT. *Geotex. Geomem.* **32**, 44–54.

Hounsfield, G. N. 1973 Computerized transverse axial scanning (tomography). *Br. J. Radiol.* **46**, 1016–1022.

Ketcham, R. A. & Carlson, W. D. 2001 Acquisition, optimisation and interpretation of X-ray computed tomographic imagery: applications to the geosciences. *Comput. Geosci.* **27** (4), 381–400.

Kjeldsen, P., Barlaz, M. A., Rooker, A. P., Baun, A., Ledina, A. & Christensena, T. H. 2002 Present and long-term composition of MSW landfill leachate: a review. *Crit. Rev. Environ. Sci. Technol.* **32** (4), 297–336.

Mees, F., Swennen, R., Van Geet, M. & Jacobs, P. 2003 Applications of X-ray computed tomography in the geosciences. *Geol. Soc. London Spec. Publ.* **215**, 1–6.

Li, Y. L., Liu, C. R., Liu, H. N. & Liu, H. Q. 2004 Testing study on permeability characteristics of unsaturated soil. *China J. Rock Mech. Eng.* **23** (22), 3861–3865 (in Chinese).

Mouser, P. J., Rizzo, D. M., Druschel, G. K., Morales, S. E., Hayden, N., O'Grady, P. & Stevens, L. 2010 Enhanced detection of groundwater contamination from a leaking waste disposal site by microbial community profiles. *Water Resour. Res.* **46**, W12506.

Otani, J., Mukunoki, T. & Obara, Y. 2000 Application of X-ray CT method for characterization of failure in soils. *Soils Founda.* **40** (2), 111–118.

Slack, R. J., Gronow, J. R., Hall, D. H. & Voulvoulis, N. 2007 Household hazardous waste disposal to landfill: using LandSim to model leachate migration. *Environ. Pollut.* **146** (2), 501–509.

Sun, D. S., Liu, P., Xia, X. H. & Wang, J. H. 2004 Permeability coefficient of unsaturated soils. *J. Hydrol. Eng.* **3** (8), 71–76 (in Chinese).

Werth, C. J., Zhang, A. Y., Brusseau, M. L., Oostrom, M. & Baumann, T. 2010 A review of non-invasive imaging methods and applications in contaminant hydrogeology research. *J. Contam. Hydrol.* **113**, 1–24.

Wittlingerova, Z., Machackova, J., Petruzelkova, A., Trapp, S., Vlk, K. & Zima, J. 2013 One-year measurements of chloroethenes in tree cores and groundwater at the SAP Mimon Site, Northern Bohemia. *Environ. Sci. Pollut. Res.* **20** (2), 834–847.

Zhelezny, P. V. & Shapiro, A. A. 2006 Experimental investigation of the diffusion coefficients in porous media by application of X-Ray computer tomography. *J. Porous Media.* **9** (4), 275–288.

First received 12 April 2013; accepted in revised form 9 December 2013. Available online 21 December 2013